ACS Energy LETTERS

Cite This: ACS Energy Lett. 2018, 3, 2240−2245

http://pubs.acs.org/journal/aelccp

LETTER

Studying the Effect of MoO_3 in Hole-Conductor-Free Perovskite Solar Cells

Eytan Avigad and Lioz Etgar*

Institute of Chemistry, Casali Center for Applied Chemistry, The Hebrew University of Jerusalem, Jerusalem 91904, Israel

Supporting Information

ABSTRACT: Owing to the superior properties of hybrid perovskite, it is possible to avoid some of the selective layers in perovksite solar cells (PSCs). One known example is the so-called hole-conductor-free PSCs, which were discovered at the beginning of the perovskite race. In this work, we introduce a thin MoO_3 layer, in HTM-free PSCs, at the perovskite/gold interface in order to investigate its influence on photovoltaic (PV) performance and to study the charge extraction behavior, recombination lifetime, and effect of hysteresis. Charge extraction measurements show that implementing a MoO_3 layer results in more charges to be extracted; this is beneficial to its PV performance. Intensity-modulated photovoltage spectroscopy shows two characteristic times at high and low frequency. The high frequency is dependent on light intensity and is related to the charge carrier recombination in the perovskite, whereas the low frequency is independent of light intensity and might be related to ion diffusion. Finally, it was observed that the MoO_3 forms a noncontinuous layer on the perovskite surface, which on the one hand improves its PV performance but on the other hand does not provide a physical barrier at this interface. This work provides new insights on HTM-free PSCs and the importance of their interfaces.

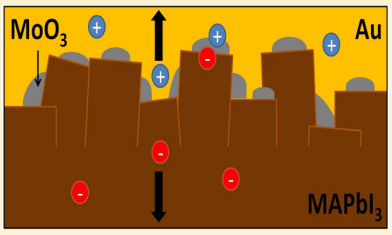

Perovskite solar cells (PSCs) have become a promising alternative to commercial solar cells, with efficiencies rapidly increasing in the past few years, reaching up to 22.7%[1] for single-junction devices. Initially an organic−inorganic $CH_3NH_3PbI_3$ ($MAPbI_3$) structure was used as a light harvester and yielded reasonable efficiencies but lacked stability; thus, some treaments and additional layers were suggested, and fully inorganic perovskite was introduced based on $CsPbI_3$.[2,3] In order to achieve high efficiency solar cell electron- and hole-transporting materials (ETM/HTM) were used, such as spiro-OMETAD and TiO_2, respectively. However, the addition of such layers in the cell complicates the production and increases the cost; in addition, more interfaces in the cell can mean more defects, leading to unwanted recombination. Hence, a HTM-free PSC[4−6] was developed and yielded reasonable efficiency. Nevertheless, the performance of HTM-free cells is not optimal; therefore, other ways of improving the HTM-free cells were investigated, such as surface passivation[7] and antisolvant treatment[8,9] after deposition in order to smooth the perovskite surface. An additional alternative is to add a thin insulating layer at the perovskite/metal contact interface. It is clear that in this solar cell structure one of the main drawbacks stems from the interface perovksite/metal contact due to the lack of a HTM layer. MoO_3 is a well-known metal oxide that has been widely studied. Several reports concluded that MoO_3 can be used as a HTM in inverted solar cell devices[10,11] or as a contact together with a low-cost metal.[12,13] Schulz et al. report on the high work function of MoO_3 and its chemical reaction with the perovksite, which results with low device performance.[14] Owing to the large band gap of MoO_3, we decided to explore the option of adding a thin (a few ∼nm) passivation layer of MoO_3 in between the perovskite and the Au back contact in HTM-free PSCs. The MoO_3 layers were deposited using thermal evaporation, with thicknesses ranging from 1.9 to 7.2 nm (as measured on Si wafers), on top of which the Au contact was evaporated. Characterization of the solar cells included *JV* curves by scanning in both directions (e.g., forward and reverse), which revealed a hysteresis effect varying slightly for each type of cell. The photovoltaic (PV) results were in good agreement with the charge extraction (CE) measurements, which allowed us to find an optimal thickness for the MoO_3 layer. A MoO_3 thickness of 1.9 nm displayed the best PV performance for the HTM-free cells, compared with the other thicknesses and in the case without a MoO_3 layer. The intensity-modulated photovoltage spectroscopy (IMVS) measurements shed more light on the electronic properties of these solar cells under different illumination intensities, predicting two lifetime characterisitcs, each corresponding to another process in the cell. We concluded that the low-frequency lifetime can be related to ion diffusion characteristics whereas the high-frequency lifetime is related to charge recombination in the perovskite.

Received: July 8, 2018
Accepted: August 25, 2018
Published: August 25, 2018

Downloaded via HEBREW UNIV OF JERUSALEM on September 17, 2018 at 08:22:16 (UTC).
See https://pubs.acs.org/sharingguidelines for options on how to legitimately share published articles.

© 2018 American Chemical Society

DOI: 10.1021/acsenergylett.8b01169
ACS Energy Lett. 2018, 3, 2240−2245

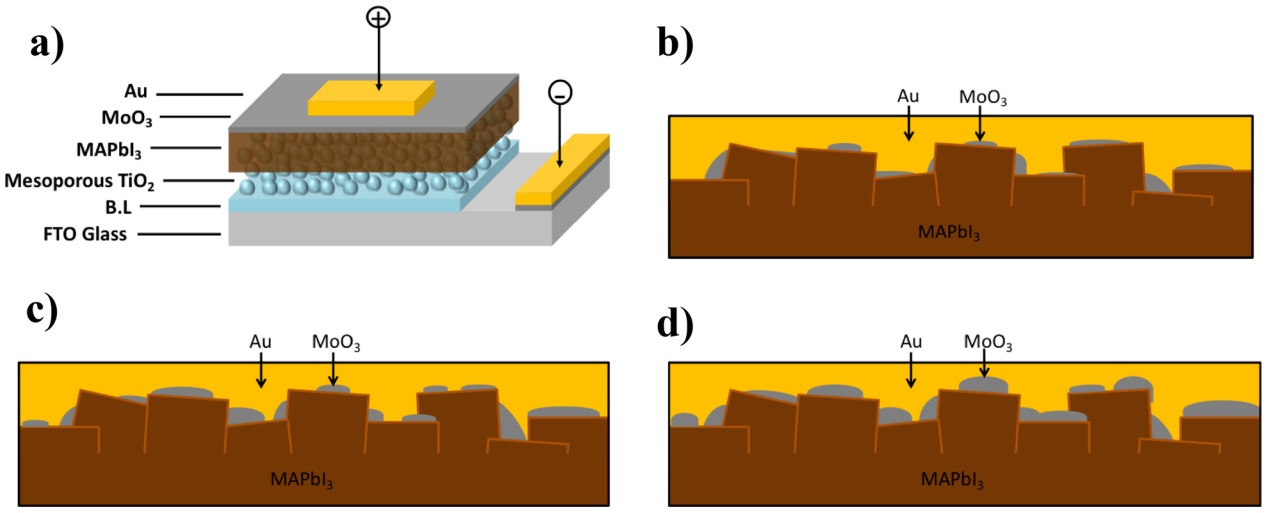

Figure 1. (a) Structure of the hole-conductor-free PSC with a thin (~nm) MoO_3 layer between the perovskite and the gold contact. (b–d) Schematic illustration of the $MAPbI_3$–MoO_3–Au interface with increasing amounts of evaporated MoO_3.

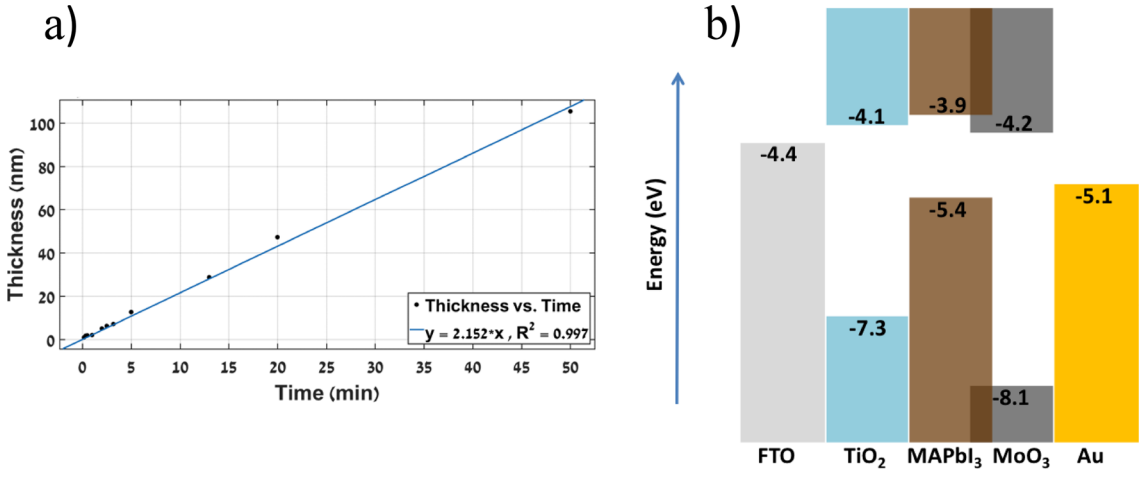

Figure 2. (a) MoO_3 thickness evaporated on Si wafers and measured using an ellipsometer. (b) Band diagram of the discussed solar cell. The MoO_3 band gap was extracted from the absorbance spectra onset; then, the Fermi level was measured by a Kelvin probe, and the relative distance of the valence band edge to the Fermi level was determined by XPS.

Our work discusses the basic structure of HTM-free PSCs, to which we introduced a thin layer of MoO_3 between the perovskite and the Au back contact, as shown in Figure 1a. The $MAPbI_3$ perovskite used here was deposited by a two-step deposition method. In this solar cell configuration, the perovskite is used as a light harvester and hole conductor at the same time. During illumination, the front contact collects the electrons that were transferred from the perovskite through the TiO_2 film (ETM), and the back contact collects the holes. It is clear that in this solar cell structure one of the main drawbacks stems from the interface perovksite/Au owing to the lack of a HTM layer. Therefore, in this work, we introduced a thin layer of MoO_3 between the perovskite and the Au. The MoO_3 was evaporated directly on the perovskite film prior to Au evaporation. In order to get an idea about the evaporated MoO_3 thickness, a calibration curve was plotted, (Figure 2a) where the MoO_3 thickness was measured by an ellipsometer on Si wafers. The *x*-axis defines the evaporation time, whereas the *y*-axis shows the measured thickness of the MoO_3 film, all of which were done on a Si wafer for calibration.

In order to determine the MoO_3 energy level position, several techniques were used. According to the absorbance measurements, the band gap of MoO_3 was 3.9 eV (Figure S3, Supporting Information). X-ray photoelectron spectroscopy (XPS) measurements were performed to determine the distance of the valence band from the Fermi level, as can be seen in Figure S2, Supporting Information. It shows that the valence band is positioned 3.4 eV from the Fermi level. In addition, the surface photovoltage spectroscopy (SPV) measurements show that the MoO_3 work function is located at 4.7 eV, which completes the picture of the energy level position of MoO_3, as presented in Figure 2b. It appears that the energy level position of MoO_3 does not permit hole transfer from perovskite to gold whereas it allows electron transfer to the gold contact. At first, this does not seem beneficial; however, when MoO_3 is deposited directly on the perovskite film, it does not create a continuous layer (as opposed to the case on the Si wafer where there was a calibration curve) probably due to the perovksite's surface roughness. As mentioned earlier, the perovksite was deposited by a two-step deposition method, which usually results in much higher roughness than does the one-step deposition method.

DOI: 10.1021/acsenergylett.8b01169
ACS Energy Lett. 2018, 3, 2240–2245

Table 1. Average PV Parameters of the HTM-Free Cells and the Champion Cells (in brackets), Obtained at Different MoO_3 Thicknesses

MoO_3 thick. (nm)	V_{oc} (V)	J_{sc} (mA/cm^2)	FF (%)	efficiency (%)	hyst. (%)
7.2	0.83 ± 0.08 (0.81)	13.5 ± 2.9 (16.8)	55 ± 6 (58)	6.2 ± 1.5 (7.9)	18.4 ± 7
6.3	0.87 ± 0.05 (0.87)	14 ± 1.4 (14.9)	55 ± 5 (62)	6.6 ± 0.8 (8.1)	13.5 ± 5.0
1.9	0.84 ± 0.07 (0.9)	13.8 ± 1.6 (17.9)	59 ± 4 (59)	6.8 ± 1.1 (9.5)	13.6 ± 7.9
no MoO_3	0.86 ± 0.07 (0.89)	13.2 ± 1.6 (16.3)	56 ± 6 (56)	6.3 ± 0.9 (8.1)	12.0 ± 5.9

Figure S1a–d, Supporting Information shows scanning electron microscopy (SEM) images of different thicknesses of MoO_3 evaporated on the perovksite surface. No indication of MoO_3 can be observed on the surface, which suggests that there is not a continuous layer of MoO_3 on the perovskite surface but rather that MoO_3 creates islands on the perovskite surface, as shown in the close-up illustrations in Figure 1b–d. Because MoO_3 is evaporated through the same shadow mask as the gold contact, we can recognize a thin film of MoO_3 on the FTO coating, which further supports the notion that the perovskite's roughness is responsible for the noncontinuous layer of MoO_3 on the perovskite surface. Figure S1e shows the MoO_3 thin film on the FTO.

The PV paremeters and the current voltage curves of the cells can be seen in Table 1 and Figure 3a, respectively. It can

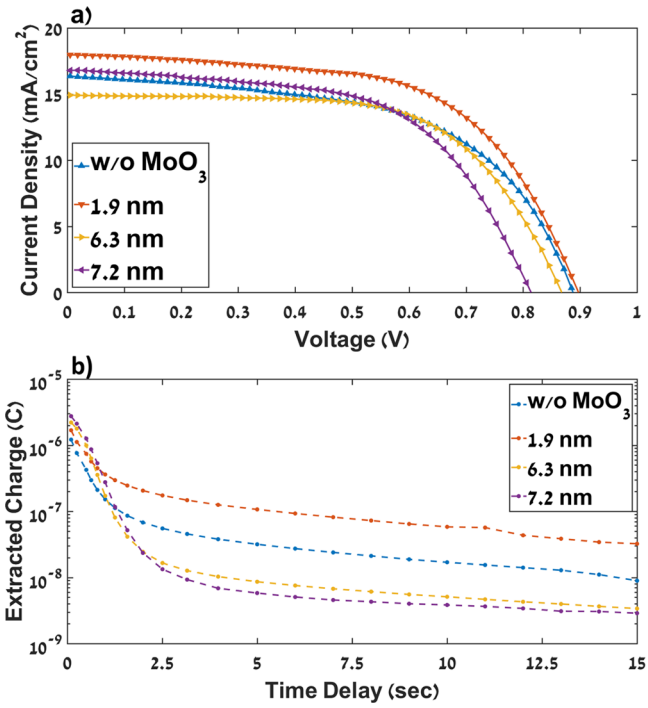

Figure 3. (a) Current–voltage (*JV*) curves of the best HTM-free cells for different MoO_3 thicknesses. (b) CE measurements of the HTM-free cells with different MoO_3 thicknesses.

be seen that 1.9 nm of MoO_3 slightly improves the cells' average performance relative to the average performance of the cells without MoO_3, whereas increasing the MoO_3 thickness beyond 1.9 nm decreases the cells' performance.

The average short-circuit current density (J_{sc}), the fill factor (FF), and the power conversion efficiency of the standard cells (w/o MoO_3) improved from 13.2 mA/cm^2, 0.56, and 6.3% to 13.8 mA/cm^2, 0.59, and 6.8% with 1.9 nm MoO_3, respectively, whereas the V_{oc} value seems to decrease with the addition of MoO_3, as might be expected due to the energy level alignment of MoO_3. The PV parameters of the champion cells under each condition can be seen in brackets in Table 1, whereas their *JV* curves are shown in Figure 3a. In this case, there is a clear cut where the 1.9 nm thickness performed better than the others, showing 9.5% efficiency for the HTM-free cell. The close average of the PV parametres for the different MoO_3 thicknesses can result from several factors such as (i) the noncontinuous layer of MoO_3 on the perovksite surface and (ii) the small variations in the MoO_3 thickness, which were studied here. When the MoO_3 thickness was increasd to more than 7.2 nm, the cells exhibited almost no PV performance, which forced us to work at this range of MoO_3 thicknesses. In addition, tracking the PV performance of the cells during time shows that no chemical reaction occurs between the MoO_3 and the perovskite (see Table S1). External quantum effciecny (EQE) measurements were performed on the solar cells with different thicknesses of MoO_3, as can be seen in Figure S4. No change was observed in the shape of the EQE between the cells.

The CE method was used to further investigate the recombination process and traps in these HTM-free solar cells. The CE measurements include the following steps: illuminating the cell for 5 s under open-circuit conditions and then short-circuiting the cell and leaving it in the dark for a certain period of time (delay time) before closing the circuit and extracting the remaining charges.

Figure 3b shows the results of the CE measurements. As seen, the cell with 1.9 nm of MoO_3 thickness has more charges left to be extracted than the standard HTM-free cell without MoO_3. This observation means that in this case there is less recombination and possibly some traps due to this additional MoO_3 thin coverage, resulting in better PV performance. With a thicker MoO_3 layer (6.3 and 7.2 nm), far fewer charges were left to be extracted. This might be attributed to the insulating nature of MoO_3, which forces the recombination to occur in the perovskite layer after illumination, resulting in decreased PV performance and, therefore, fewer charges to be extracted.

IMVS was used to study the recombination behavior in this solar cell structure with different MoO_3 thicknesses. In this technique, the cell was illuminated with modulated light (frequencies of 1–10^5 Hz). When measuring the transfer function, we could find the impedance of the cell and assign an equivalent circuit to it. When plotting the impedance in the complex plane, we could see two semicircles forming at both a high range of frequencies (10^2–10^3 Hz) and lower frequencies (1–10 Hz). By finding the minimum of the semicircle, we could calculate the characteristic lifetime. The IMVS measurement was repeated for different light intensities ranging from 0.1 to 0.7 Sun.

The first time characteristic was found at high frequencies (10^2–10^3 Hz), which correspond to liftimes on the order of 0.1–1 ms and are associated with the charge carriers' recombination in the perovskite layer. It shows an exponential decay with increasing light intensity, which is directly related to

DOI: 10.1021/acsenergylett.8b01169
ACS Energy Lett. 2018, 3, 2240–2245

the charge carriers' density in the perovskite (Figure 4a). As can be seen, this characteristic lifetime is not influenced by the

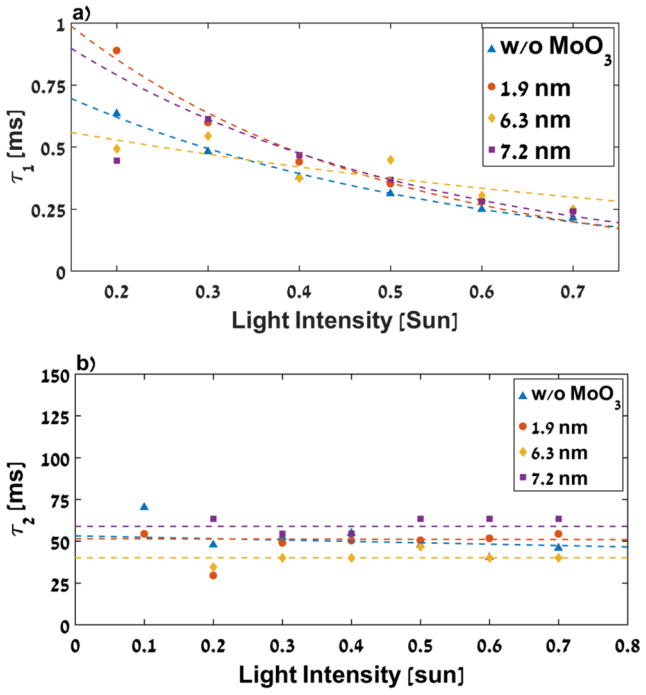

Figure 4. (a) First recombination lifetime obtained at high frequencies (10^2–10^3 Hz) with different light intensities. (b) Second characteristic time obtained at low frequencies (1–10 Hz) with different light intensities.

MoO_3 thickness; therefore, it can be assumed that it is related to the TiO_2/perovskite interface, which is responsible for this recombination behavior.

The second characteristic lifetime is observed at low frequencies when measuring IMVS (1–10 Hz), and it is on the order of 10–100 ms and remains relatively constant throughout all of the light intensities (Figure 4b). The same observation was reported by Zarazua et al.,[15] who recognized a constant time characteristic as a function of the light intensity and the fact that the capacitive element and the resistive element behave in opposite ways with respect to light intensity, which leads to a constant characteristic time. Because this time characteristic is independent of the light intensity, it can be associated with surface charge accumulation at the interface.[16,17] This light-independent characteristic is an indication of the coupling between the resistance and the surface recombination capacitance. We can assume that this characteristic time is linked to the reported ionic movment, as was also previously predicted.[18]

Current–voltage measurements were performed in both directions, from 1.2 to −0.1 V (reverse scan), and then immediately measured at forward scans, from low voltage to high voltage. A decrease in the cell PV performance was observed; this pehnomenon is known in the literature as hysteresis.[19,20]

Figure 5 shows the reverse and forward scan results (hysteresis loops) of cells that achieve average PV performance for each MoO_3 thickness. The loop is not completely closed according to the definition because the V_{oc} value from the forward scan is ∼10 mV lower than the reverse scan value, V_{oc}, and the J_{sc} value from the reverse scan is ∼0.5 mA/cm^2 higher. This fact is worth mentioning because our calculation of the hysteresis effect is different from previous reports. The confined area between the two curves displays the energy loss of the solar cells resulting from hysteresis. The smallest hyseteresis is obtained with the standard solar cells (without MoO_3) and it increases with increased MoO_3 thickness. However, the differences in the hysteresis loss are small for the 1.9 and 6.3 nm MoO_3 thicknesses, whereas for 7.2 nm it increases further. We calculated the energy loss using the following equation, as we recently reported[21]

$$P = \sum_{j=0}^{J_{sc}} (j \cdot dv) \qquad \%\text{Hysteresis} = \frac{P_{reverse} - P_{forward}}{P_{reverse}} \cdot 100 \tag{1}$$

To calculate the power (P) of each cell, we used eq 1; as shown above, the current density (j) was summed and multiplied by the voltage step (dv = 0.0131 V), and the forward scan power was subtracted from the reverse scan power to obtain the total hysteresis loss. The values obtained from the calculation are shown in Table 1.

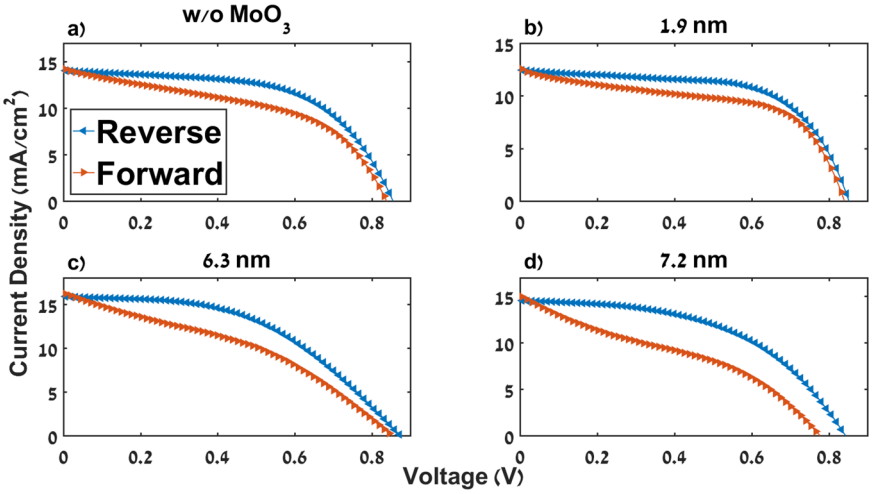

Figure 5. *JV* curves of average cells with increased amounts of MoO_3. Scanning backward then forward gives a hysteresis loop that is more pronounced in cells with 6.3 and 7.2 nm (c,d) of MoO_3 than the cells without MoO_3 and with 1.9 nm (a,b).

DOI: 10.1021/acsenergylett.8b01169
ACS Energy Lett. 2018, 3, 2240–2245

This hysteretic behavior in PSCs is highly affected by charge accumulation at the interfaces;[22] therefore, in standard configurations, such as mesoporous and inverted PSC structures, hole- and electron-selective contacts are used to improve the charge transfer. MoO_3 can create trap states for charges at the interface (supported by the CE as well) with Au and, therefore, can result in higher energy loss (e.g., larger hysteresis values). Importantly, hysteresis can be affected by the number of scans, where continuous scanning of *JV* usually minimizes the hysteresis. In these experiments, we carefully measured each cell, i.e., one time a forward scan and immediately after one time a reverse scan; multiple scans were not performed.

In this work, we evaporated MoO_3 at the perovskite/gold interface in hole-conductor-free PSCs. Conventional $MAPbI_3$ perovskite deposited in two steps was used to investigate how the MoO_3 layer influences these HTM-free cells' PV performance, CE, recombination lifetime, and the hysteresis mechanism. Carefull characterization showed that MoO_3 is evaporated as a noncontinuous layer on the surface, and therefore, it does not provide physical blocking at this interface. We found that with a 1.9 nm thickness of MoO_3 the PV performance was the highest, supported by the CE measurements. Interestingly, the IMVS measurements revealed two time characteristics: (1) the high-frequency time characteristic, which decreases with light intensity and is associated with the charge carriers' recombination in perovskite, and (2) the low-frequency time characteristic, which is independent of the light intensity and is associated with ion diffusion. Finally, we calculated the energy loss resulting from the hysteresis effect in those cells that display a small difference in hysteresis for HTM-free cells without MoO_3 and for the thinnest MoO_3 layer. This study elaborates more on the investigation of HTM-free cells and provides a possible route to improve their PV performance.

■ ASSOCIATED CONTENT

Supporting Information

The Supporting Information is available free of charge on the ACS Publications website at DOI: 10.1021/acsenergylett.8b01169.

Experimental section, including SEM, XPS, EQE, and UV−vis spectrophotometry measurements (PDF)

■ AUTHOR INFORMATION

Corresponding Author

*E-mail: lioz.etgar@mail.huji.ac.il.

ORCID

Lioz Etgar: 0000-0001-6158-8520

Notes

The authors declare no competing financial interest.

■ ACKNOWLEDGMENTS

We would like to thank the Israel Ministry of Energy for financial support and Dr. Monika Rai for the EQE measurements.

■ REFERENCES

(1) Yang, W. S.; Park, B.-W.; Jung, E. H.; Jeon, N. J.; Kim, Y. C.; Lee, D. U.; Shin, S. S.; Seo, J.; Kim, E. K.; Noh, J. H.; Seok, S. I. Iodide Management in Formamidinium-Lead-Halide-Based Perovskite Layers for Efficient Solar Cells. *Science* **2017**, *356*, 1376−1379.

(2) Eperon, G. E.; Paterno, G. M.; Sutton, R. J.; Zampetti, A.; Haghighirad, A. A.; Cacialli, F.; Snaith, H. J. Inorganic Caesium Lead Iodide Perovskite Solar Cells. *J. Mater. Chem. A* **2015**, *3*, 19688−19695.

(3) Nam, J. K.; Chai, S. U.; Cha, W.; Choi, Y. J.; Kim, W.; Jung, M. S.; Kwon, J.; Kim, D.; Park, J. H. Potassium Incorporation for Enhanced Performance and Stability of Fully Inorganic Cesium Lead Halide Perovskite Solar Cells. *Nano Lett.* **2017**, *17*, 2028−2033.

(4) Etgar, L.; Gao, P.; Xue, Z.; Peng, Q.; Chandiran, A. K.; Liu, B.; Nazeeruddin, M. K.; Grätzel, M. Mesoscopic CH3NH3PbI3/TiO2 Heterojunction Solar Cells. *J. Am. Chem. Soc.* **2012**, *134*, 17396−17399.

(5) Laban, W. A.; Etgar, L. Depleted Hole Conductor-Free Lead Halide Iodide Heterojunction Solar Cells. *Energy Environ. Sci.* **2013**, *6*, 3249−3253.

(6) Aharon, S.; Gamliel, S.; Cohen, B. E.; Etgar, L. Depletion Region Effect of Highly Efficient Holeconductor Free CH3NH3PbI3 Perovskite Solar Cells. *Phys. Chem. Chem. Phys.* **2014**, *16*, 10512−10518.

(7) Noel, N. K.; Abate, A.; Stranks, S. D.; Parrott, E. S.; Burlakov, V. M.; Goriely, A.; Snaith, H. J. Enhanced Photoluminescence and Solar Cell Performance via Lewis Base Passivation of Organic−Inorganic Lead Halide Perovskites. *ACS Nano* **2014**, *8*, 9815−9821.

(8) Cohen, B. E.; Aharon, S.; Dymshits, A.; Etgar, L. Impact of Antisolvent Treatment on Carrier Density in Efficient Hole-Conductor-Free Perovskite-Based Solar Cells. *J. Phys. Chem. C* **2016**, *120*, 142−147.

(9) Xiao, M.; Huang, F.; Huang, W.; Dkhissi, Y.; Zhu, Y.; Etheridge, J.; Gray-Weale, A.; Bach, U.; Cheng, Y.; Spiccia, L. A Fast Deposition-Crystallization Procedure for Highly Efficient Lead Iodide Perovskite Thin-Film Solar Cells. *Angew. Chem., Int. Ed.* **2014**, *53*, 9898−9903.

(10) Hou, F.; Su, Z.; Jin, F.; Yan, X.; Wang, L.; Zhao, H.; Zhu, J.; Chu, B.; Li, W. Efficient and Stable Planar Heterojunction Perovskite Solar Cells with an MoO3/PEDOT:PSS Hole Transporting Layer. *Nanoscale* **2015**, *7*, 9427−9432.

(11) Ali, F.; Khoshsirat, N.; Duffin, J. L.; Wang, H.; Ostrikov, K.; Bell, J. M.; Tesfamichael, T. Prospects of e-Beam Evaporated Molybdenum Oxide as a Hole Transport Layer for Perovskite Solar Cells. *J. Appl. Phys.* **2017**, *122*, 123105.

(12) Zhao, Y.; Nardes, A. M.; Zhu, K. Effective Hole Extraction Using MoOx-Al Contact in Perovskite CH3NH3PbI3 Solar Cells. *Appl. Phys. Lett.* **2014**, *104*, 213906.

(13) Sanehira, E. M.; Tremolet de Villers, B. J.; Schulz, P.; Reese, M. O.; Ferrere, S.; Zhu, K.; Lin, L. Y.; Berry, J. J.; Luther, J. M. Influence of Electrode Interfaces on the Stability of Perovskite Solar Cells: Reduced Degradation Using MoOx/Al for Hole Collection. *ACS Energy Lett.* **2016**, *1*, 38−45.

(14) Schulz, P.; Tiepelt, J. O.; Christians, J. A.; Levine, I.; Edri, E.; Sanehira, E. M.; Hodes, G.; Cahen, D.; Kahn, A. High-Work-Function Molybdenum Oxide Hole Extraction Contacts in Hybrid Organic-Inorganic Perovskite Solar Cells. *ACS Appl. Mater. Interfaces* **2016**, *8*, 31491−31499.

(15) Zarazua, I.; Han, G.; Boix, P. P.; Mhaisalkar, S.; Fabregat-Santiago, F.; Mora-Seró, I.; Bisquert, J.; Garcia-Belmonte, G. Surface Recombination and Collection Efficiency in Perovskite Solar Cells from Impedance Analysis. *J. Phys. Chem. Lett.* **2016**, *7*, 5105−5113.

(16) Almora, O.; Zarazua, I.; Mas-Marza, E.; Mora-Sero, I.; Bisquert, J.; Garcia-Belmonte, G. Capacitive Dark Currents, Hysteresis, and Electrode Polarization in Lead Halide Perovskite Solar Cells. *J. Phys. Chem. Lett.* **2015**, *6*, 1645−1652.

(17) Juarez-Perez, E. J.; Sanchez, R. S.; Badia, L.; Garcia-Belmonte, G.; Kang, Y. S.; Mora-Sero, I.; Bisquert, J. Photoinduced Giant Dielectric Constant in Lead Halide Perovskite Solar Cells. *J. Phys. Chem. Lett.* **2014**, *5*, 2390−2394.

(18) Yang, T.; Gregori, G.; Pellet, N.; Grätzel, M.; Maier, J. The Significance of Ion Conduction in a Hybrid Organic-Inorganic Lead-Iodide-Based Perovskite Photosensitizer. *Angew. Chem.* **2015**, *127*, 8016−8021.

DOI: 10.1021/acsenergylett.8b01169
ACS Energy Lett. 2018, 3, 2240−2245

(19) Snaith, H. J.; Abate, A.; Ball, J. M.; Eperon, G. E.; Leijtens, T.; Noel, N. K.; Stranks, S. D.; Wang, J. T.-W.; Wojciechowski, K.; Zhang, W. Anomalous Hysteresis in Perovskite Solar Cells. *J. Phys. Chem. Lett.* **2014**, *5*, 1511−1515.
(20) Chen, B.; Yang, M.; Priya, S.; Zhu, K. Origin of J−V Hysteresis in Perovskite Solar Cells. *J. Phys. Chem. Lett.* **2016**, *7*, 905−917.
(21) Iagher, L.; Etgar, L. Effect of Cs on the Stability and Photovoltaic Performance of 2D/3D Perovskite-Based Solar Cells. *ACS Energy Lett.* **2018**, *3*, 366−372.
(22) Wu, B.; Fu, K.; Yantara, N.; Xing, G.; Sun, S.; Sum, T. C.; Mathews, N. Charge Accumulation and Hysteresis in Perovskite-Based Solar Cells: An Electro-Optical Analysis. *Adv. Energy Mater.* **2015**, *5*, 1500829.

DOI: 10.1021/acsenergylett.8b01169
ACS Energy Lett. 2018, 3, 2240−2245